A raman study of energy transfer processes between phonon and vibron in RDX and β-HMX at low temperatures

Shuji Ye*, Kenichi Tonokura*, and Mitsuo Koshi*

The Raman spectra of some phonon and vibron modes in RDX (hexahydro-1, 3, 5-trinitro-1, 3, 5-triazine) and β-HMX (octahydro-1, 3, 5, 7-teranitro-1, 3, 5, 7-tetrazocine) crystals have been measured at temperatures ranging from 3.8K to 300.0K. Shifts in phonon frequency decreased with increasing temperature under high vacuum conditions. It is found that phonons and vibrons have similar averaged lifetime (6.8ps for phonon modes and 4.0ps for vibron modes). The bandwidths of phonons and vibrons increased with increasing temperatures. The temperature dependence of bandwidth γ was fitted to a functional form of correct. This temperature dependence was interpreted in terms of three-phonon down process as well as of dephasing processes. Three-phonon and dephasing processes are the dominant relaxation mechanism for most of vibrons.

1. Introduction

When a molecular crystal receives a shock (or impact), a part of mechanical energy is transferred from the shock to the lattice vibration (phonons). Phonon energy then must be converted to molecular vibrations, in order to heat them up to a temperature at which a chemical bond can be broken. This energy transfer process, which termed as multiphonon up pumping [1], is expected to be the rate-determining step for the explosion. However, information on the energy transfer rates between phonons and vibrons (molecular vibrations) is very limited.

Raman spectroscopy [2] is proved to be a useful tool to obtain information on the lifetimes of phonons and vibrons and their relaxation processes. In a molecular crystal, due to the occurrence of anharmonic phonon-phonon or phonon-vibron interactions, phonon energy will transfer to another phonons or vibrons. In a perfect crystal, the total relaxation time T_2 is determined by the superposition of two different mechanisms, a population decay process characterized by a lifetime T_1 and a pure dephasing process with a lifetime T_2^* [3]. The total dephasing time T_2 is given by [4][5]

$$\frac{1}{T_2} = \frac{1}{T_2^*} + \frac{1}{2T_1} \tag{1}$$

The bandwidth γ of the Raman spectral line is related to the total lifetime T_2:

$$\gamma = \frac{1}{\pi c T_2} \tag{2}$$

where c is the speed of light. The experimental information obtained from the temperature dependence of the bandwidth provides the clue for identifying the dominant mechanisms involved in the overall relaxation. According to equation (1), the bandwidth γ can be expressed as a sum of the contributions from population decay processes and a pure dephasing process as follows [6][7]:

Received: March 7, 2002
Accepted: March 12, 2002
*Department of Chemical System Engineering, The University of Tokyo, 7−3−1 Hongo, Bunkyo-ku, Tokyo 113-8656, JAPAN
TEL: +81-3-5841-7295
FAX: +81-3-5841-7488
E-mail: Koshi@chemsys.t.u-tokyo.ac.jp

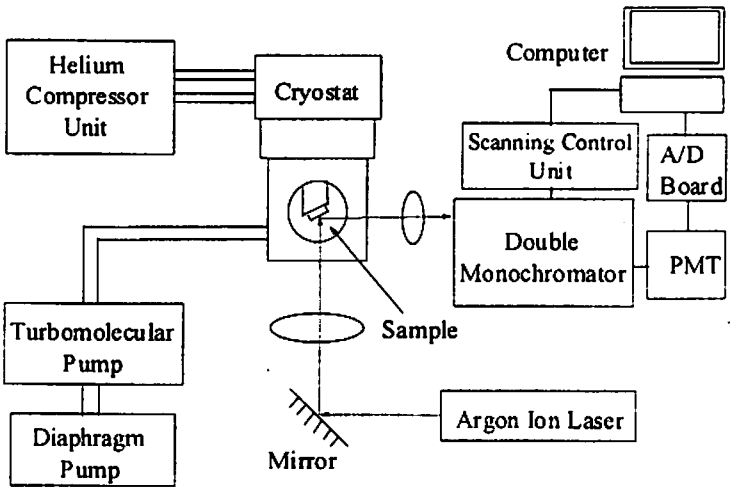

Fig.1 Schematic of low temperature Raman spectroscopy apparatus.

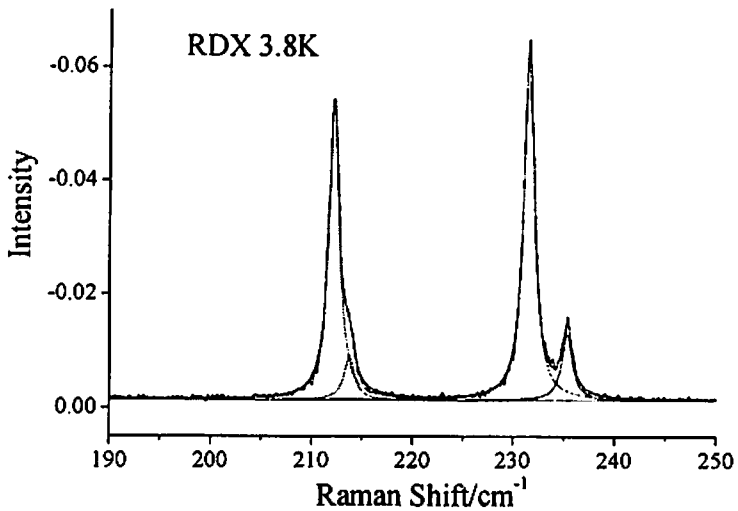

Fig.2 An example of Lorentzian fitting results.

$$\gamma = \gamma_{3d} + \gamma_{3u} + \gamma_{deph},$$
$$\gamma_{3d} = B_{3d}(n_i + n_j + 1),$$
$$\gamma_{3u} = B_{3u}(n_i - n_j), \qquad (3)$$
$$\gamma_{deph} = B_{deph} n_i (n_i + 1).$$

Here, B_{3d} and B_{3u} are third-order anharmonic terms of the crystal Hamiltonian for the three-phonon processes, in which the initial phonon energy $h\omega$ will transfers to two phonons having energies of $h\omega_i$ and $h\omega_j$. For the three-phonon down process (B_{3d}), energies of both final phonon states are less than initial phonon energy ($\omega > \omega_i, \omega_j$), whereas for the three-phonon up process, one of the final phonon state has higher energy than initial phonon energy ($\omega_j > \omega > \omega_i$). B_{deph} is a forth-order anharmonic term of the crystal Hamiltonian for the dephasing process. Here, the energy of the final state $h\omega_i$ should be very close to the initial phonon energy. n_i is the occupation number of the i-th phonon mode and given by

$$n_i = [\exp(h\omega_i / kT) - 1]^{-1} \qquad (4)$$

It is noted that the contributions from γ_{3u} and γ_{deph} vanish and $\gamma = \gamma_{3d}$ at T=0. Therefore we can determine the lifetime (or energy transfer rate) for the three-phonon population decay from the bandwidth at T=0. In addition, at the temperature region of $h\omega < kT$, the bandwidths caused by population decay processes (γ_{3d} and γ_{3u}) depend linearly on the temperature, while the bandwidth is proportional to T^2 for the dephasing process.

In the present paper, we measured the shifts and bandwidths of some Raman active lattice phonons and vibrons in RDX and β-HMX crystals. Lifetimes for the three-phonon down process were determined by the extrapolation of the bandwidths to T=0. Contributions from population decay and dephasing processes were separated on the basis of the temperature dependence of the bandwidths of Raman spectral lines.

2. Experimental

All spectra were recorded using a double monochromator (CT-1000D, Japan Spectroscopic Co., Ltd) with a Coherent Innova70-5 continuous wave argon-ion laser. The laser was tuned to 514.5 nm with a power output of 0.25~0.45W. Monochromator slit widths were set at 50 μm, which resulted in a spectral resolution of 0.2 cm^{-1}. Spectra from 10 to 3100 cm^{-1} at 3.9K and 300.0K were recorded with a scan speed of 100 cm^{-1} /min, while some of the spectral lines were recorded with a scan speed of 10 cm^{-1}/min at high vacuum condition (<10^{-3}Pa). Samples were cooled down to 3.5 K using Cryogenic refrigerator for optical measurements (PS24SS, Nagase Co.; Ltd, Japan). The temperature of the sample was equilibrated before the Raman spectrum was recorded. A schematic of the experimental apparatus is shown in Fig.1. The noise of signal in spectra was reduced using a digital filter. Line shape of the Raman spectra was fitted to a Lorentzian function, and the line position and bandwidth were determined. An example of the Lorentzian fitting was shown in Fig2.

The samples were obtained from the Chugoku Corporation of Chemical Pharmacy, Japan, and the recrystallization of the samples was performed three times from saturated ethanol/acetone solution. The typical sizes of RDX and β-HMX crystals are 2.0×2.0×1.5mm and 1.5×1.5×1.0mm, respectively

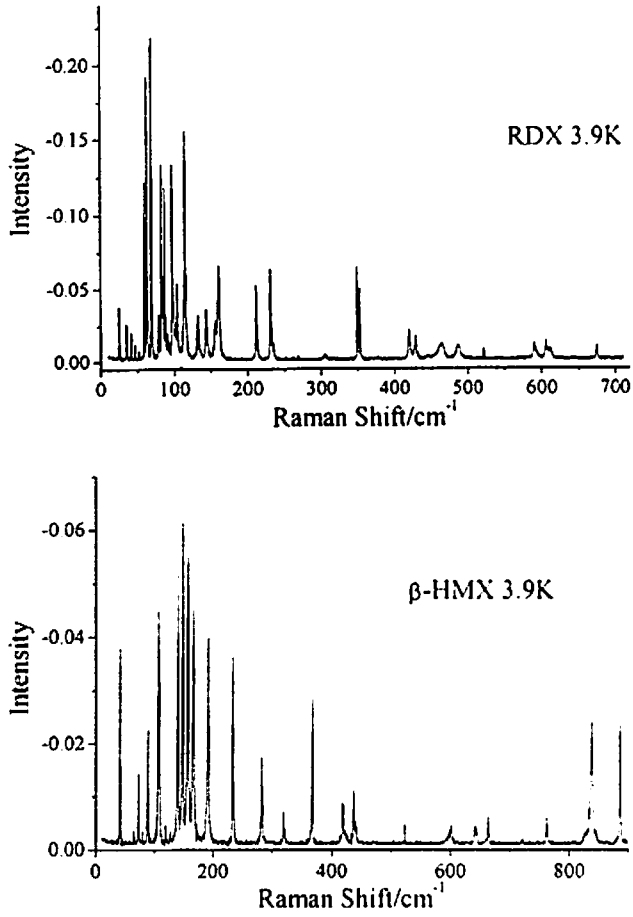

Fig.3 Raman Spectrum of RDX and b-HMX crystals at 3.9K.

3. Results and discussion

3.1 Raman spectra at 3.9K

The Raman spectra in the region of 10~3100cm^{-1} of RDX and β-HMX crystal at 3.9K are shown in Fig.3(a) and (b). At low temperatures, total of 70 and 60 lines were observed for RDX and β-HMX, respectively, rather than 57×8 and 39×2 modes that predicted by the factor group analysis. Some lines in the vibron region split into two peaks. These splitting may be caused by the factor-group splitting (such as Davydov effect). Vibrational frequencies and their assignments are given in Table 1 for the split lines observed in RDX spectra.

In RDX crystal the lattice is built with pairs of eight inverted interlocked molecules[8) 11)]. In the pair structure, intermolecular electrostatic interactions are important because of the alternating relative positive and negative charge on the atoms in RDX. The oxygen atoms and amine nitrogen atoms are negatively polarized while the carbon atoms and nitrogen atoms positively polarized [12)]. One of the oxygen atoms of the axial N-NO_2 groups situates in the molecular "pocket" [11)] of the neighboring molecule and attractively interacts with all three nitrogen atoms of the nitro groups. Other oxygen atoms attract neighboring pairs of molecules by interaction with nitro-nitrogen of the equatorial N-NO_2 group. Thus cohesion exists between all of the RDX mol-

Table1 Splitting of some vibrons in RDX crystal.

ν /cm^{-1} at 300.0K	ν /cm^{-1} at3.9K		ν_{calc} /cm^{-1}[a]	Sym.[a]	Assignment[a]
	Peak1	Peak2			
149.4	156.5	161.2	153	A″	t (NO_2), δ(NN)
207.9	212.4	213.7	200	A′	γ(NN), α_N, τ
227.5	231.6	235.4	220	A″	γ(NN)
349	350.0	353.5	311	A′	δ(NO_2), ν (NN), δ(NN), α_C, α_N
740.3	737.1	740.8	742	A′	r(NO_2), δ(NN)
759.5	759.9	760.9	731	A″	r(NO_2), δ(NN)
789.6	791.2	792.2	796	A′	ω(NO_2), r, R, α
1277.9	1279.0	1282.3	1286	A″	ν_s(NO_2), ν(NN), t, δ(NO_2)
1573.7	1572.6	1575.1	1559	A″	ν_a(NO_2), r(NO_2)
{1595.4 1601.0	{1596.0 1602.7	1597.3	} 1603	A′	ν_a(NO_2), r(NO_2), ω

a). Reference 9 and 10

ecule pairs because of the oxygen affinity. But the intermolecular forces between the molecular pairs are weak [13], and the interaction between RDX molecular pairs is expected to play an important role to this kind of Davydov splitting, which can be proved by the fact that the splitting only occurs in these modes assigned to the deformation N-N and NO_2, referred to Table 1 and Fig.2. In this case, the molecular vibrational modes do not behave as independent uncoupled units [14]. Further study is required to clarify the origin of these splitting.

In β-HMX crystal, as analyzed by Brill [15], the dominant intermolecular interactions are offset to some extent by one of O···N repulsion and another O···N attraction combined with one of O···O repulsion. These coupling interactions result splitting in some vibrational modes while others behave as nearly independence uncoupled units.

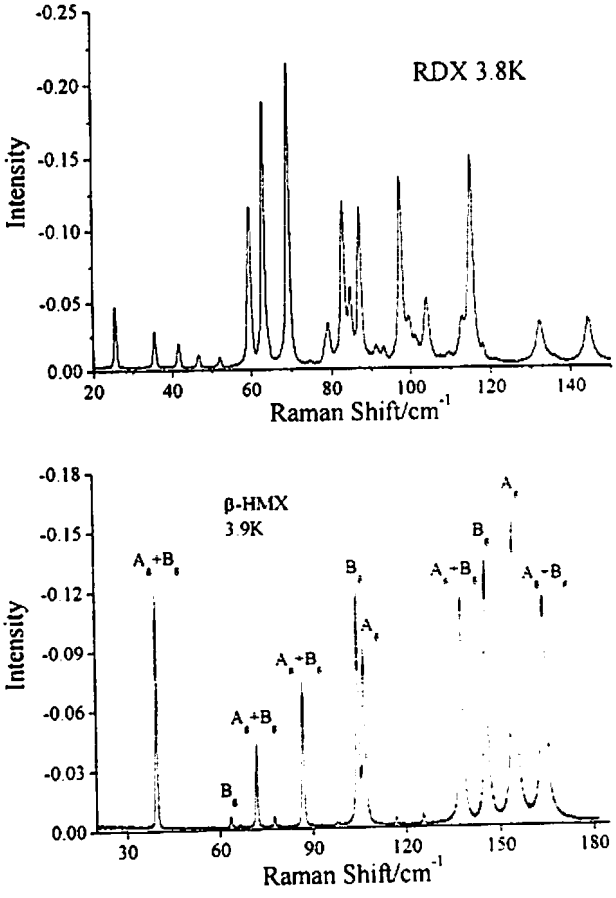

Fig.4 Raman Spectra in the lattice mode region at low temperature.

3.2 Lattice modes

The Raman spectra in the lattice mode region are shown in fig.4. For RDX, Raman peaks are observed at 21.7, 30.0, 51.9, 61.2, 72.5 cm^{-1} at 300.0K while these peaks shift and split into 25.7, 35.6, 41.6, 46.7, 52.1, 59.7, 63.3, 69.5, 74.5, 79.1, 83.1, 84.9, 87.3, 91.2 and 93.3 cm^{-1} at 3.8K. According to the factor group analysis, RDX should have 24 phonon modes ($6A_g$+$6B_{1g}$+$6B_{2g}$+$6B_{3g}$), but not all of these modes could be observed, which indicates some phonon modes overlap with together.

For β-HMX, its phonon mode spectrum is relatively simple. At room temperature, Raman lines are observed at 36.0 and 65.0 cm^{-1} at 300.0K. They have both A_g and B_g symmetry. At the temperature of 3.9K, two peaks shift to 39.5 and 71.8 cm^{-1}. In addition, at 3.9 K, we observed weak peaks at 63.5 and 125.3 cm^{-1}, the former should be 58cm^{-1} at room tem-

Table2 Low-temperature frequency and bandwidths of phonon modes of RDX

ν(0K)/cm^{-1}	γ/cm^{-1}	T_1/ps	B	C
25.7	0.6	8.9	0.009	2.0×10^{-5}
35.6	0.7	7.6	0.015	1.2×10^{-5}
41.7	0.7	7.6	0.011	4.5×10^{-5}
46.9	0.6	8.9	0.018	1.5×10^{-5}
52.1	0.6	8.9	0.008	5.2×10^{-5}
59.9	1.0	5.3	0.012	1.22×10^{-4}
63.6	0.8	6.7	0.025	5.3×10^{-5}
69.7	0.9	5.9	0.021	2.3×10^{-5}
115.3	1.3	4.1	0.011	5.4×10^{-5}
144.6	2.0	2.7	0.014	3.9×10^{-5}

Table3 Low-temperature frequency and bandwidths of phonon modes of β-HMX

Sym.[a)]	ν(0K) /cm^{-1}	γ/cm^{-1}	T_1/ps	B	C	Assignment[a)]
A_g+B_g	39.5	0.5	10.7	0.008	1.3×10^{-5}	Librational
B_g	63.5	0.5	10.7	——	——	Librational
A_g+B_g	71.8	0.5	10.7	0.016	3.1×10^{-5}	Librational
A_g+B_g	87.1	0.6	8.9	0.017	2.0×10^{-5}	γ(N-N)+τ (ring)
B_g	104.5	0.8	6.7	0.008	1.15×10^{-4}	γ(N-N)+τ (ring)
A_g	106.8	0.9	5.9	0.016	5.4×10^{-5}	γ(N-N)+τ (ring)
A_g+B_g	137.9	1.2	4.4	0.019	3.9×10^{-5}	τ (NO_2)
B_g	145.8	1.3	4.1	0.015	4.1×10^{-5}	τ (NO_2)
A_g	154.6	1.7	3.1	0.017	2.9×10^{-5}	τ (NO_2)
A_g+B_g	164.3	2.1	2.5	0.018	3.8×10^{-5}	τ (NO_2)

a) Reference 17

perature reported by Cavagnat et al [16]. They assigned this peak to B_g symmetry. There is no report about the latter peak.

RDX and β-HMX have very low frequency vibrational modes involving NO_2 rocking motions, which lie below phonon maximum cutoff frequency (Ω_{max}) These vibrations do not act as doorway modes. The doorway mode is defined as the vibrational mode whose frequency is larger than phonon maximum-cutoff frequency (Ω_{max}) and less than $2\Omega_{max}$. Those modes having lower frequency than Ω_{max} are "amalgamated" in the phonon modes. They are expected to behave much like phonons in that they will be directly excited by the shock [1]. For this reason, we assign these modes as phonon modes.

The low-temperature frequencies and bandwidths of some phonon modes of RDX and β-HMX have been measured. The results are listed in Table 2 and 3. Phonon modes of RDX have lifetimes T_1 ranging from 2.7 to 8.9 ps with the averaged lifetime of 6.7 ps. In β-HMX, the lifetimes T_1 of phonon modes are in the range of 2.5~10.7 ps with the averaged lifetime of 6.8ps.

The frequencies of all the phonon modes depend on temperature. It is found that these frequencies could be fitted to a functional form of $\nu(T)=\nu(0)-BT-CT^2$. The mode at 63.6cm^{-1} of RDX has a maximum frequency change of 11.0cm^{-1} between 3.8 and 300.0K. The mode at 106.8cm^{-1} of β-HMX has a maximum frequency change of about 9cm^{-1}. The frequency dependence on the temperatures under high vacuum condition is different with the results under high pressure condition where the frequencies show a normal linear decrease with increasing temperature [18]. Under the high vacuum condition, the crystal lattice spacing is largely increasing with temperatures than that under pressured conditions. Two examples of the bandwidths as a function of temperature are shown in Fig.5. Some of them (35.6 and 63.6cm^{-1} in RDX, 87.1 and 137.9cm^{-1} in β-HMX) de-

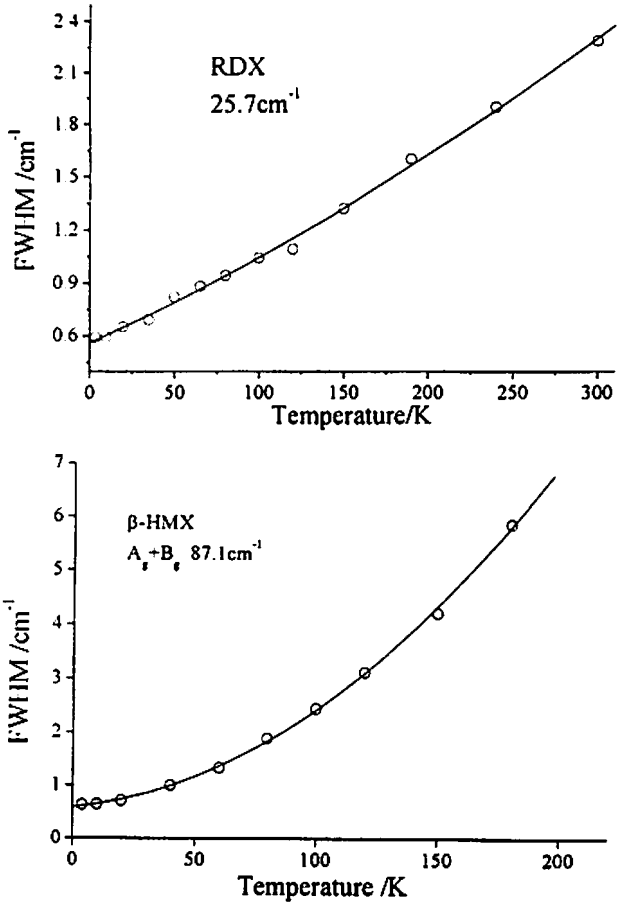

Fig.5 Examples of phonon- bandwidths dependence with temperature for phonons.

pend on temperature as T^2, whereas others (25.7, 59.9, 69.7 and 115.3cm^{-1} in RDX, 39.5, 71.8, 104.5, 106.8, 145.8,154.6 and 164.3cm^{-1} in β-HMX) are linearly dependent on temperatures at region of $h\omega<\kappa T$.

3.3 Vibron modes

Raman shifts and bandwidths of several vibrons of RDX and β-HMX have been measured as a function of temperatures. The low temperature frequencies and bandwidths of these vibrons are listed in Table 4 and 5, and the lifetimes T_1 of vibron are summarized in Table 6. RDX and β-HMX have almost the same averaged lifetime (about 4 ps), which is in good agreement with the results of Fayeret al. [19] Fayer and his co-workers have measured the relaxation rates of asymmetric stretching mode (~1580cm^{-1}) of nitro-group for several explosives at room temperature using infrared pump-probe experiments.

The vibrational frequency shifts in RDX crystals show T^2 dependence, whereas shifts in β-HMX crystal are insignificant. With the exception of some bands, a general feature of the vibron bandwidths as a function of temperature is their nonlinear behavior in the temperature range of $h\omega<\kappa T$, which is a typical signature of the occurrence of fourth order or dephasing processes. Temperature dependence in the bandwidths is mainly given by the temperature dependence of the phonon and vibrational population as given by eq.3. Although the assignments of the energy levels (i.e., i and j in eq.(3)) are not unique [20], most probable processes can be identified by taking into account measured phonon frequencies. The simplest fourth order process is the dephasing process, which is expected to be the most efficient for vibron relaxation. It can dephase the vibrons within their own dispersion curves

For molecular vibrations, relaxation can occur either to the lower frequency (down process) or to higher frequencies (up-pumping process)[1]. In the

Table4 Low-temperature frequency and bandwidths of vibron modes of RDX crystal

Sym.	ν /cm^{-1}	γ /cm^{-1}	T_1 /ps	Assignment[a)]
A′	212.4	1.3	4.1	γ (NN), α_N, τ
A′	213.7	1.2	4.4	γ (NN), α_N, τ
A″	231.6	1.4	3.8	γ (NN)
A″	235.4	1.3	4.1	γ (NN)
A′	350.0	1.0	5.3	δ(NO_2), ν (NN), δ(NN), α_C, α_N
A′	353.5	0.9	5.9	δ(NO_2), ν (NN), δ(NN), α_C, α_N
A′	675.0	1.7	3.1	δ(NO_2), r,ω(NO_2), α_C
A′	852.0	1.8	3.0	ω(NO_2),
A″	861.4	0.7	7.6	ω(NO_2),
A′	887.6	2.0	2.7	R, δ(NO_2),ν(NN)

a). Reference 9 and 10

Table5 Low-temperature frequency and bandwidths of vibron modes of β-HMX crystal*

Sym[a].	ν /cm^{-1}	γ /cm^{-1}	T_1 /ps	Assignment[a]
B_g	231.8	1.1	4.8	Ring
A_g	234.0	1.0	5.3	Ring
A_g+B_g	281.0	2.0	2.7	Ring
A_g+B_g	365.4	1.4	3.8	Ring
A_g+B_g	885.2	1.6	3.3	Ring (stretch)
A_g+B_g	957.2	2.6	2.0	Ring (stretch)
B_g	971.6	1.0	5.3	Ring (stretch)
A_g	973.5	0.8	6.7	Ring (stretch)
A_g+B_g	1171.1	1.4	3.8	Ring (stretch)
A_g+B_g	1354.4	2.3	2.3	γ or τ (CH_2)
A_g+B_g	1368.6	2.1	2.5	γ or τ (CH_2)
A_g+B_g	1418.1	1.4	3.8	δ (CH_2)
B_g	1436.8	1.7	3.1	δ (CH_2)
A_g	1439.0	1.9	2.8	δ (CH_2)
A_g+B_g	1456.2	1.6	3.3	δ (CH_2)
A_g+B_g	1463.3	1.4	3.8	δ (CH_2)

a) Reference 17

Table6 Lifetime (ps) of phonon and vibron modes of explosives.

Explosives	RDX	β-HMX
Impact sensitivity (h_{50}/cm)	24	26
Phonon modes	2.7~8.9(6.7)	2.5~10.7(6.8)
vibron modes	2.6~8.1(4.4)	2.0~6.7(3.7)
The result (~1580cm^{-1}) of Fayer[9]	6.2±0.4ps	4±1ps

The value in () is the averaged lifetime.

Table7 Anharmonic coefficients and phonon frequencies for the vibron relaxation process in RDX crystal*.

Sym.	ν /cm^{-1} (300.0K)	B_{3d}	ω_1 /cm^{-1}	ω_2 /cm^{-1}	B_{doph}	ω /cm^{-1}
A″	108.5	1.28	30(P)	78(P)	—	—
A′	207.9	1.25	150(P)	58(P)	0.055	20(P)
A″	227.5	1.35	150(P)	78(P)	0.06	20(P)
A′	348.3	0.97	301(D)	47(P)	0.02	20(P)
A′	350.8	0.93	301(D)	50(P)	0.02	20(P)
A′	671.3	1.67	593(V)	78(P)	0.034	20(P)
A′	849.5	1.77	740(V)	109(P)	0.013	20(P)
A″	859.3	0.66	790(V)	69(P)	—	—
A′	886.5	2.02	790(V)	97(P)	0.0175	20(P)

*P = phonon; D = doorway vibration; V = high frequency vibrational mode.

down processes, a part of the vibron energy has to be transferred to phonons. In the up-pumping processes, vibron has to gain energy from phonon. According to the energy levels of phonons and vibrons in RDX and β-HMX spectra, energy transfer processes of vibrons have been interpreted using expression of eq.3 by assuming that they relax to a vibrational mode of lower energy level and create a

Table8 Anharmonic coefficients and phonon frequencies for the vibron relaxation process of β-HMX crystal*.

Sym.	v /cm^{-1} (300.0K)	B_{3d}	ω_1 /cm^{-1}	ω_2 /cm^{-1}	B_{deph}	ω /cm^{-1}
B_g	96	0.80	48(P)	48(P)	—	—
A_g	97	0.92	48(P)	49(P)	—	—
A_g+B_g	130	1.20	65(P)	65(P)	0.07	36(P)
B_g	138	1.25	48(P)	90(P)	—	—
A_g	148	1.70	58(P)	90(P)	—	—
A_g+B_g	156	2.10	59(P)	97(P)	—	—
B_g	231	1.06	152(P)	79(P)	0.045	36(P)
A_g	231	1.0	152(P)	79(P)	0.07	36(P)
A_g+B_g	280	2.0	183(D)	97(P)	0.095	36(P)
A_g+B_g	362	1.35	231(D)	131(P)	0.07	36(P)
A_g+B_g	884	1.60	755(V)	129(P)	0.034	36(P)
A_g+B_g	1170	1.42	1088(V)	82(P)	0.085	36(P)
A_g+B_g	1417	1.35	1320(V)	97(P)	0.01	36(P)

*P = phonon; D = doorway vibration; V = high frequency vibrational mode.

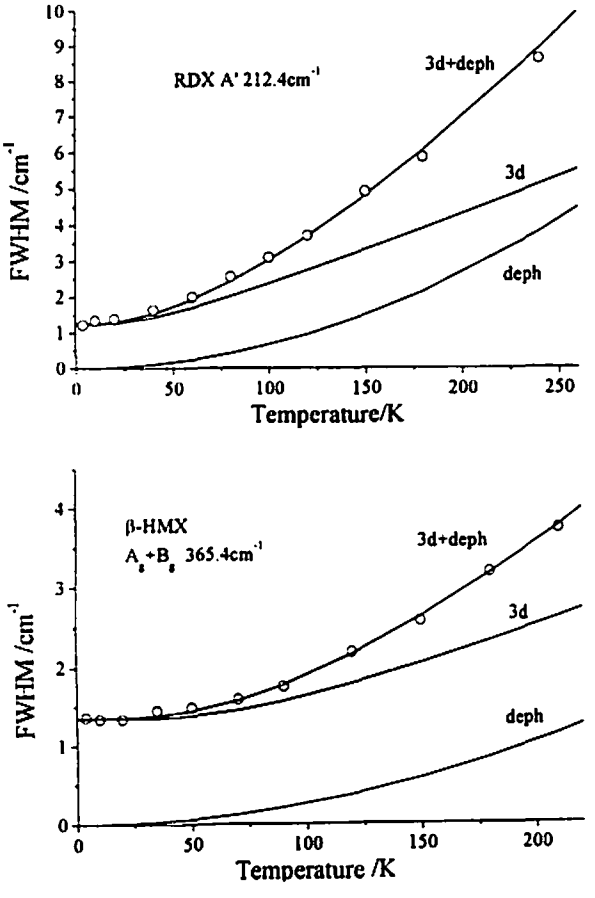

Fig.6 Temperature dependence of bandwidths of some vibron modes; open cycle: experimental data; solid lines: theoretical fitting. 3d= three-phonon down process; deph=pure dephasing process; 3d+deph = sum of the contributions of 3d and deph processes.

phonon (three-phonon down process). At the same time, low energy-level phonon has an interaction with the vibron by a dephasing process. For example, the mode at 207.9cm^{-1} of RDX relaxes to the mode at 150cm^{-1} and creates a phonon (58cm^{-1}), and at the same time, the phonon at 20 cm^{-1} interacts with it by dephasing process. As for the doorway vibrations, they relax themselves by phonon-phonon (P-P) or doorway vibration-phonon (D-P) mechanism. The higher frequency vibrational modes relax through vibron-phonon (V-P) mechanism. The relaxation results were shown in Table 7 and 8 and in Fig.6. As can be seen, three-phonon down and dephasing processes are the dominant relaxation mechanism for most of vibrational bands.

4. Conclusion

In the present study, temperature dependences of shifts and bandwidths of RDX and β-HMX Raman spectra have been measured. Splitting of some vibron modes at low temperature was observed. Shifts in phonon frequencies of RDX and β-HMX depend on temperature as T^2. The lifetimes of some phonons and vibrons for the population relaxation processes were estimated on the basis of the bandwidths at 0K.. It is found that these explosives have almost the same averaged lifetime for the population relaxation.

Temperature dependence of the bandwidths of vibrons is interpreted in terms of three- phonon down as well as of dephasing processes. It is concluded that the three-phonon down and dephasing processes are the dominant relaxation processes for most of vibrational bands.

To understand the initiation mechanism of shock-induced detonation, it is necessary to know the rate of the population relaxation from phonon to vibron for many molecules including insensitive explosives. Results of present study indicated that the life times of phonons and vibrons at T=0 K are almost same for RDX and HMX. It is interesting to investigate the lifetime of insensitive explosives. The energy transfer rate is not only dependent on the lifetime at T=0 K, but also dependent on the density of states for final phonon or vibron states. Therefore it is also required to calculate the density of states for phonons and vibrons. Such studies are currently in progress in our laboratory.

Ackow ledgement

Authors are galeful to Mr. Kitajima (Chugoku-kayaku) for his help to obtain RDX and ITMX nred in the present work.

Reference

1) A.Tokmakoff, M.D. Fayer, and D.D. Dlott, J.Phys.Chem. 97: 1901 (1993).
2) P. Foggi, and V. Schettino, Rivista Del Nuovo Cimento, 15: 1 (1992).
3) S. Califano, V. Schettino, and N. Neto, Lattice dynamics of molecular crystals, vol.26 in Springer series on Lecture notes in Chemistry, edited by G. Berthier, et al. (Springer, Berlin, 1981).
4) S. Califano, and V. Schettino, Int.Rev.Phys. Chem. 7:19 (1988).
5) S. Califano, in Applied Laser Spectroscopy, Vol.241 in NATO ASI Series B Physics, edited by W. Demtröder, and Inguscio (Plenum, New York, 1990).
6) E.F. Archibong, and A.J. Thakkar, Chem.Phys. Lett. 201,485 (1993).
7) E. Burgos, C.S. Murthy, and R. Righini, Mol. Phys. 47:1391 (1982).
8) C.S. Choi, and E. Prine. Acta Crystallogr. B28: 2857 (1972).
9) M. Rey-Lafon, C. Trinquecoste, R.Cavagnat, and M.T.Forel, J. Chim. Phys. 68: 1533 (1971).
10) A. Trinquecoste, M. Rey-Lafon, and M.T. Forel, J. Chim. Phys. 72: 689 (1975).
11) R.J. Karpowicz, and T.B. Brill, J. Phys. Chem. 87: 2109 (1984).
12) M.K. Orloff, P.A. Mullen, and F.C. Rauch, J. Phys.Chem. 74: 2189 (1970).
13) F.Goetz, and T.B.Brill, J.Phys. Chem. 83:340 (1979).
14) R.J. Karpowicz, R.J. and T.B. Brill, J. Phys. Chem. 88: 348 (1984).
15) T.B. Brill, C.O. Reese, J. Phys. Chem. 84: 1376 (1980)
16) M.R. Cavagnat, M.T. Forel, M. Rey. Lafon, C.R. Acad. Sci. B273: 658 (1971).
17) Z. Iqbal, S. Bulusu, J.R. Autera, J. Chem. Phys. 60:221 (1974)
18) F.J. Owens, and Z. Iqbal, J. Chem. Phys. 74: 4242 (1981).
19) A.M. Aubuchon, K.D. Rector, W. Holmes, and M.D. Fayer, Chem. Phys. Lett. 299:84 (1999)
20) M. Becucci, E. Castellucci, P. Foggi, S. Califano, and D.A. Dows, J Chem. Phys. 96: 98 (1992)